Journal of Medicinal Chemistry

Article

pubs.acs.org/jmc

3,6-Diamino-4-(2-halophenyl)-2-benzoylthieno[2,3-*b*]pyridine-5-carbonitriles Are Selective Inhibitors of *Plasmodium falciparum* Glycogen Synthase Kinase-3

Wiebke Fugel,[†] Anselm Erich Oberholzer,[‡] Bernhard Gschloessl,[§] Ron Dzikowski,[∥] Narkiss Pressburger,[∥] Lutz Preu,[†] Laurence H. Pearl,[⊥] Blandine Baratte,[#] Morgane Ratin,[#] Ilya Okun,[▽] Christian Doerig,[○] Sebastian Kruggel,[◆] Thomas Lemcke,[◆] Laurent Meijer,*[,#,¶] and Conrad Kunick*[,†]

[†]Institut für Medizinische und Pharmazeutische Chemie, Technische Universität Braunschweig, Beethovenstrasse 55, 38106 Braunschweig, Germany

[‡]Structural Biology Community Laenggasse (sbcl), 3000 Bern, Switzerland

[§]Centre de Biologie pour la Gestion des Populations (CBGP), UMR1062, Institut National de la Recherche Agronomique (INRA), Campus International de Baillarguet, CS 30016, 34988 Montferrier-sur-Lez, France

[∥]Department of Microbiology & Molecular Genetics, The Kuvin Center for the Study of Infectious and Tropical Diseases, Institute for Medical Research Israel-Canada (IMRIC), The Hebrew University-Hadassah Medical School, Jerusalem 91120, Israel

[⊥]Genome Damage and Stability Centre, School of Life Sciences, University of Sussex, Brighton BN1 9RH, United Kingdom

[#]Protein Phosphorylation & Human Disease Group, CNRS USR 3151, Station Biologique, Place Georges Teissier, 29680 Roscoff, France

[▽]Research & Development, ChemDiv, Inc., 6605 Nancy Ridge Drive, San Diego, California 92121, United States

[○]Department of Microbiology, School of Biomedical Sciences, Monash University, Wellington Road, Clayton, Victoria 3800, Australia

[◆]Institut für Pharmazie, Universität Hamburg, Bundesstrasse 45, 20146 Hamburg, Germany

[¶]ManRos Therapeutics, Perharidy Research Center, 29680 Roscoff, Bretagne, France

Supporting Information

ABSTRACT: *Plasmodium falciparum* is the infective agent responsible for malaria tropica. The glycogen synthase kinase-3 of the parasite (*Pf*GSK-3) was suggested as a potential biological target for novel antimalarial drugs. Starting from hit structures identified in a high-throughput screening campaign, 3,6-diamino-4-(2-halophenyl)-2-benzoylthieno[2,3-*b*]pyridine-5-carbonitriles were discovered as a new class of *Pf*GSK-3 inhibitors. Being less active on GSK-3 homologues of other species, the title compounds showed selectivity in favor of *Pf*GSK-3. Taking into account the X-ray structure of a related molecule in complex with human GSK-3 (*Hs*GSK-3), a model was computed for the comparison of inhibitor complexes with the plasmodial and human enzymes. It was found that subtle differences in the ATP-binding pockets are responsible for the observed *Pf*GSK-3 vs *Hs*GSK-3 selectivity. Representatives of the title compound class exhibited micromolar IC_{50} values against *P. falciparum* erythrocyte stage parasites. These results suggest that inhibitors of *Pf*GSK-3 could be developed as potential antimalarial drugs.

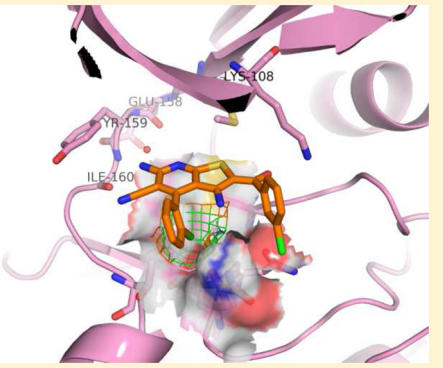

INTRODUCTION

Malaria is one of the most severe infectious diseases worldwide, affecting mainly the poor population in developing countries. Young children in tropical African countries are particularly threatened by *Plasmodium falciparum*, the parasite causing the most virulent form of malaria. Although the use of insecticide-treated mosquito nets has resulted in a significant reduction in the number of infections in several countries, there were still 225 million malaria cases reported in 2009, 781 000 of which ended fatally.[1] A major problem of malaria therapy is the limited number of suitable drugs and the development of resistance. While older medications such as chloroquine or pyrimethamine have become ineffective against *P. falciparum* due to resistance in most endemic regions, the current standard therapy consists of an artemisinin derivative combined with a second antiplasmodial drug.[2,3] Recent reports of *P. falciparum* decreased susceptibility against artemisinin from the Cambodia−Thailand border are alarming.[1,4] Further propagation of artemisinin resistance could compromise the progress achieved in the fight against malaria in

Received: October 25, 2012

   dx.doi.org/10.1021/jm301575n | *J. Med. Chem.* XXXX, XXX, XXX−XXX

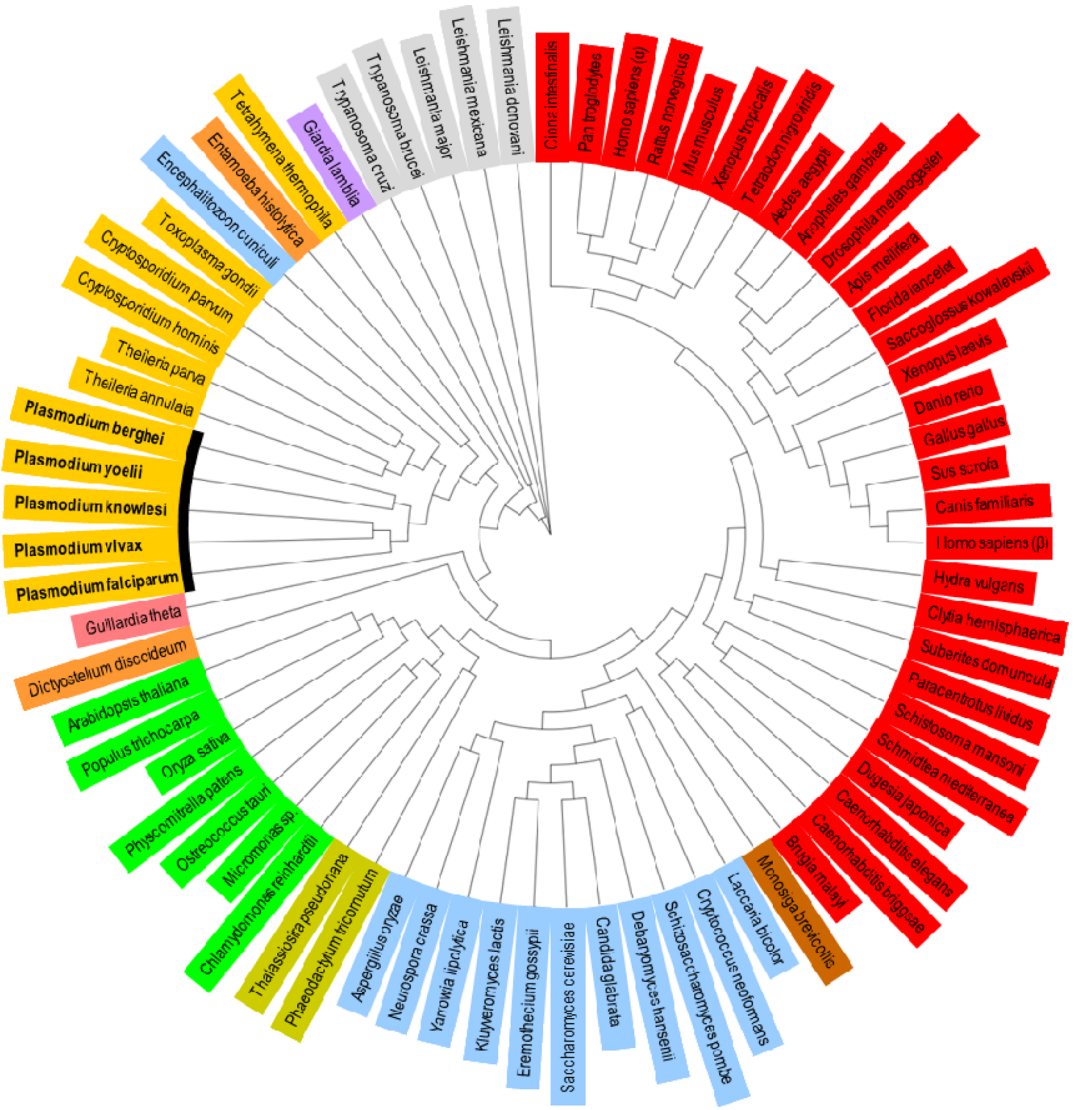

Figure 1. Sequence analysis of GSK-3 orthologues in 71 species. Phylogenetic tree according to the GSK-3 sequence. The set of 71 GSK-3 proteins is composed of sequences presented in the orthoMCL database (http://www.orthomcl.org)[36] and orthologues which were recovered by bidirectional BLAST (*blastp*) analyses of the GSK3 human isoforms against the specific species reference protein set. Multiple alignments were created with ClustalW (version 2.0.10)[37] and were manually improved afterward. The phylogenetic tree itself was built with the maximum likelihood approach implemented in PHYML (version 3.0).[38,39] As amino acid substitution, the LG model[40] was chosen. To obtain confidence estimates in the tree topologies, a bootstrap analysis with 1000 was applied. The consensus tree was visualized with the application Forester (http://www.phylosoft.org/forester). Color codes are as given in the Supporting Information, Figure S2. *Plasmodium* GSK-3 is given in bold.

recent years. As a consequence, there is an urgent need for additional antimalarial drugs which ideally should act on novel biological targets and/or should represent novel chemotypes. In a recent study published by Gamo et al., a collection of nearly 2 million compounds from the GlaxoSmithKline inventory were screened against in vitro cultivated *P. falciparum*, more than 13 000 compounds of which inhibited the growth of parasites in a 2 μM concentration.[5] Interestingly, the fraction of molecules presumably acting by inhibiting protein kinases was considerably higher among the hit compound group compared to all screened compounds. The authors concluded that protein kinase inhibitors might be a rich source of antimalarial drug leads in the future.[4−6] The selective inhibition of microbial protein kinases has repeatedly been suggested as a therapeutic strategy.[7−15] However, of the published examples of rationally developed inhibitors against *Plasmodium* protein kinases (e.g., *Pf*nek-1,[16,17] *Pf*PK7,[18,19] *Pf*mrk,[20−25] and *Pf*CDPK1[26]), none, to our best knowledge, have entered a clinical evaluation stage. In a previous paper the *P. falciparum* glycogen synthase kinase-3 (*Pf* GSK-3) was characterized.[27] Although its biological functions are not yet identified, *Pf* GSK-3 was demonstrated as an essential enzyme for completion of the asexual erythrocytic cycle of the parasite[28] and thus suggested as a putative antimalarial drug target.[27] In a model using *Plasmodium berghei*-infected mice, it was recently shown that the GSK-3 inhibitor lithium suppressed erythrocytic parasitemia and protected the animals against malaria.[29] In a recent paper, the identification of inhibitors of the GSK-3 homologue of *Trypanosoma brucei*, the parasite causing African sleeping sickness, was reported.[30] Although none of the identified compounds showed absolute selectivity for *Tb*GSK-3 against a panel of approximately 40 human kinases, some showed antitrypanosomal activity in submicromolar concentrations and a reasonable safety window when tested on human MRC-5 cells. The authors concluded that these

dx.doi.org/10.1021/jm301575n | *J. Med. Chem.* XXXX, XXX, XXX−XXX

compounds are promising starting points for an antitrypanosomal drug development program.[30] Aiming at the development of new antimalarial drugs, the campaign reported here was directed toward identification of small molecular *Pf*GSK-3 inhibitors displaying a certain degree of selectivity over mammalian *Pf*GSK-3 orthologues.

RESULTS

Identification of 3-Amino-4-arylthieno[2,3-*b*]pyridines as *Pf*GSK-3 Inhibitors by High-Throughput Screening. A preliminary study reported the interaction of both plasmodial and mammalian GSK-3 with a selection of established kinase inhibitors.[27] Indeed, some entities (e.g., indirubin-3′-monoxime, hymenialdisine) showed *Pf*GSK-3 inhibition, however without selectivity against the porcine GSK-3 homologue (*Ss*GSK-3). This was found to also be the case for other reference kinase inhibitors (Supplementary Table S1, Supporting Information). In contrast, several members of the paullone family[31−33] of GSK-3 inhibitors showed a strong selectivity for inhibition of the mammalian GSK-3. Although the latter finding was disappointing at first sight, we concluded that the mammalian and the plasmodial homologues are sufficiently divergent to enable selectivity. Furthermore, a meticulous comparison of the ATP-binding site architectures of *Pf*GSK-3 and its human orthologue by bioinformatic methods revealed differences that warranted a search for *Pf*GSK-3-selective chemotypes.[34,35] Given the strong conservation of GSK-3 across evolution, we analyzed a selection of 71 GSK-3 orthologues of various species (Figure 1; Supplementary Table S2, Supporting Information). The results showed that GSK-3 orthologues tended to group into clusters of their taxonomic origin such as metazoa, fungi, and green plants. The only exceptions were GSK-3 proteins of *Entamoeba histolytica* (Amoebozoa) and *Encephalitozoon cuniculi* (fungi), which were arranged with the Apicomplexa group. The analyzed GSK-3 proteins to all five *Plasmodium* species cluster separately from GSK-3 orthologues, suggesting that inhibitors specific for GSK-3 from *Plasmodium* species might be identified. In addition, the recent formal demonstration that *Pf*GSK-3 is absolutely required for the survival of the erythrocytic stage of *P. falciparum* validates *Pf*GSK-3 as a potential therapeutic target.[28]

We therefore set up a high-throughput screening (HTS) in which 10 480 compounds (about half of which were kinase directed) were evaluated at a concentration of 10 μM against recombinant *Pf*GSK-3, which was previously shown to be active in in vitro kinase assays.[27] Only 18 molecular entities were found to be active (>50% inhibition at 10 μM), representing a rather modest hit rate of 0.17%. Compounds displaying more than 50% inhibition were re-evaluated by determination of IC_{50} values against *Pf*GSK-3 and against the native mammalian (porcine) *Ss*GSK-3. Interestingly, five of these inhibitors shared a common heterocyclic ring system as the parent scaffold, namely, the 3-amino-4-arylthieno[2,3-*b*]pyridine motif **3**. Two examples, **1** and **2**, of these initial hits are depicted in Chart 1.

We then tested a small focused library of 427 compounds related to **3** for *Pf*GSK-3 inhibition. Although the majority of the compounds were inactive, some showed selective activity for *Pf*GSK-3 with IC_{50} values in the micromolar concentration range, as exemplified by congener **4**.[41]

Stimulated by these preliminary results, we initialized a program for molecular modification of **4** with the aim of gaining information on structure−activity relationships and of increasing the *Pf*GSK-3 inhibitory activity and selectivity. In this context we synthesized the four groups of derivatives illustrated in Chart 2,

Chart 1. Hits 1 and 2 from the Initial Test Run, Parent 3-Amino-4-arylthieno[2,3-*b*]pyridine Scaffold 3, and Hit Structure 4 Identified from the Focused ChemDiv Library Based on Scaffold 3[a]

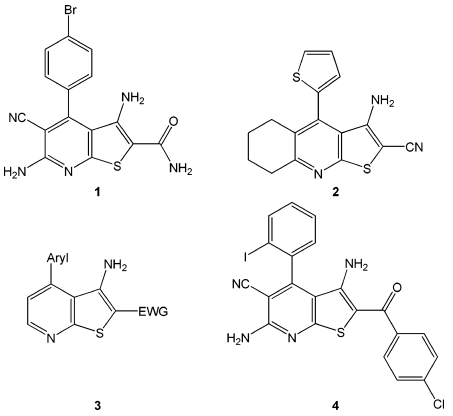

[a]Kinase inhibitory activities (IC_{50}, μM): (**1**) *Pf*GSK-3, 3.0; *Ss*GSK-3, 7.0; (**2**) *Pf*GSK-3, 9.0; *Ss*GSK-3, >10.0; [**4** (resynthesized material)] *Pf*GSK-3, 1.61; *Ss*GSK-3, >100.0.

Chart 2. 3-Amino-4-arylthieno[2,3-*b*]pyridines 5−8 Designed as Analogues of Hit Structure 4[a]

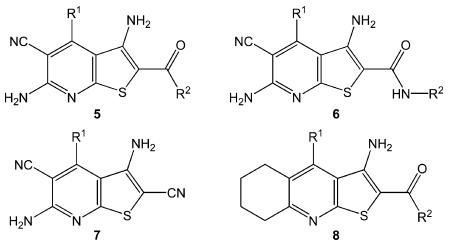

[a]For substituents R^1 and R^2, refer to Table 1.

namely, **5**, in which the substitution pattern at the phenyl rings of hit compound **4** is varied, **6**, in which, by insertion of a nitrogen atom, the aromatic ketone moiety is changed to a carboxamide (analogous to hit compound **1**), **7**, in which the benzoyl substituent is replaced by a cyano group (crossover design based on **2** and **4**), and **8**, in which the amino and cyano groups at the pyridine ring are replaced by annulation of a cyclohexene ring (crossover design based on **2** and **4**).

At the start of the synthesis program, the hit structure **4** was compared with the commercially available analogue **5dd** (Table 1) distinguished only by the lack of the *o*-iodo substituent present in **4**. Since **5dd** was completely devoid of activity against either *Pf*GSK-3 or *Ss*GSK-3, we (1) concluded that the mentioned ortho substitution was important for kinase inhibitory activity and (2) because iodo substituents are undesirable in drug molecules, paid special attention to a replacement of this element in the projected series **5**−**8**.

Chemistry. The precursor molecules **12**−**20** were synthesized from suitable aromatic aldehydes **9**, malonodinitrile **10**, and cyanothioacetamide **11** in a modified one-pot procedure analogous to the method described by Sharanin et al.[42] (Scheme 1).

Subsequently, the desired 3-amino-4-(2-haloaryl)thieno[2,3-*b*]pyridines **5**−**7** were prepared employing a successive one-pot S-alkylation/Thorpe−Ziegler cyclization methodology.[43−45] Initially, the 2-thioxo-1,2-dihydropyridines **12**−**20** were dissolved in DMF, deprotonated by 1 equiv of potassium hydroxide,

dx.doi.org/10.1021/jm301575n | J. Med. Chem. XXXX, XXX, XXX−XXX

Table 1. Structures and Kinase Inhibitory Activities of 3-Amino-4-arylthieno[2,3-*b*]pyridines 5−8

compd	R^1	R^2	IC_{50}(*Pf*GSK-3)^{a,b} (μM)	IC_{50}(*Ss*GSK-3)^{a,b} (μM)
5a	2-MeOPh	Ph	6	>100
5b	2-MeOPh	4-ClPh	>10	>10
5c	2-MeOPh	4-MeOPh	>10	>10
5d	2-MeOPh	4-MePh	>10	>10
5e	2-MeOPh	4-CF_3Ph	>10	>10
5f	2-MeOPh	3-ClPh	8.5	>10
5g	2-MeOPh	2-ClPh	>10	>10
5h	2-MeOPh	4-CNPh	>10	>10
5i	2-IPh	Ph	2.4	>10
5j	2-IPh	4-MeOPh	1.7	>10
5k	2-IPh	4-MePh	3.2	>10
5l	2-IPh	4-CF_3Ph	>10	>10
5m	2-IPh	3-ClPh	0.91	>10
5n	2-IPh	2-ClPh	>10	>10
5o	2-IPh	3,4-Cl_2Ph	70	>100
5p	2-EtOPh	4-ClPh	>10	>10
5q	2-BrPhe	Ph	1.1	>10
5r	2-BrPhe	4-ClPh	>100	>100
5s	2-BrPhe	3-ClPh	0.61	>10
5t	2-BrPhe	3,4-Cl_2Ph	3.8	>10
5u	2-thienyl	3-ClPh	>10	>10
5v	2-ClPhe	3-ClPh	0.48	>10
5w	2-ClPhe	3,4-Cl_2Ph	2.7	>10
5x	2-ClPhe	3-MeOPh	1.7	>10
5y	2-ClPhe	3-CF_3−Ph	2.2	>10
5z	2-ClPhe	3-CNPh	0.5	>10
5aa	2-ClPhe	3-BrPh	0.91	>10
5bb	2-ClPhe	3-FPh	>100	>100
5cc	2-FPhe	3-ClPh	10	>100
5dd	Ph	4-ClPh	>100	>100
6a	2-IPh	4-ClPh	>10	>10
6b	2-BrPh	4-ClPh	>10	>10
6c	2-ClPh	4-ClPh	>10	>10
7a	2-MeOPh		>10	>10
7b	2-IPh		>10	>10
7c	2-BrPh		0.8	1.3
7d	2-ClPh		0.13	0.4
7e	2-EtOPh		>10	>10
7f	2-MePh		0.51	2
7g	2-thienyl		0.18	2.3
7h	3-indolyl		1.6	3.5
8a	2-IPh	Ph	>10	>10
8b	2-IPh	4-ClPh	>10	>10

^{a}IC_{50} values were calculated from dose−response curves. The highest inhibitor concentration used in the assays was either 10 or 100 μM. Recombinant *Pf*GSK-3 and native, affinity-purified *Ss*GSK-3 were used in the studies. ^{b}All data points for construction of dose−response curves were recorded in triplicate. Typically, the standard deviation of single data points was below 10%.

Scheme 1. Synthesis of 2-Thioxo-1,2-dihydropyridines 12−20[a]

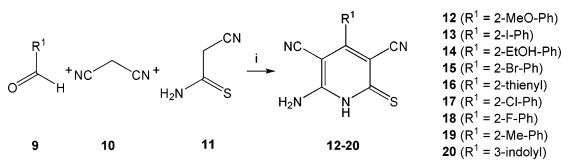

[a]Reagents and conditions: (i) EtOH, piperidine, reflux, 3 h, 21−61%.

and then S-alkylated by means of a suitable haloalkane, **21**, **22**, or **23**. The resulting thioether was not isolated, but cyclized by addition of a second equivalent of base. Depending on the nature of the haloalkane and the 2-thioxo-1,2-dihydropyridine, completion of the reaction at room temperature required between 30 min and 6 h (Scheme 2).

Following a modified protocol originally reported by Elnagdi,[46] the 3-amino-4-aryl-5,6,7,8-tetrahydrothieno[2,3-*b*]-quinolines **8a,b** were prepared in a two-step procedure from cyclohexanone (**24**) and 2-cyano-3-(2-iodophenyl)-2-propene-thioamide (**25**). The resulting 4-(2-iodophenyl)-2-thioxo-1,2,5,6,7,8-hexahydroquinoline-3-carbonitrile (**26**) underwent Thorpe−Ziegler ring closure after S-alkylation by suitable phenacyl bromides **21** and treatment with alkali (Scheme 3).

Biological Evaluation and Discussion. The compounds listed in Table 1 were evaluated in vitro by measuring the IC_{50}

dx.doi.org/10.1021/jm301575n | J. Med. Chem. XXXX, XXX, XXX−XXX

Scheme 2. Synthesis of 3,6-Diamino-4-arylthieno[2,3-*b*]pyridine-5-carbonitriles 5−7[a]

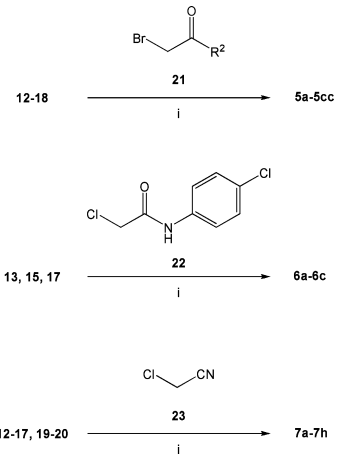

[a]Reagents and conditions: (i) (1) DMF, 1 equiv of KOH, rt, 30 min, (2) DMF, 1 additional equiv of KOH, rt, TLC monitoring, 15−91%.

Scheme 3. Synthesis of 3-Amino-4-aryl-5,6,7,8-tetrahydrothieno[2,3-*b*]quinolines 8a,b[a]

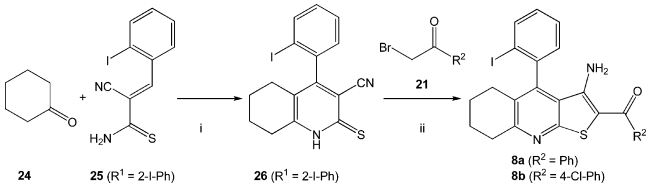

[a]Reagents and conditions: (i) 1,4-dioxane, piperidine, 80 °C, 2−4 h, TLC monitoring, 37−43%; (ii) (1) DMF, 1 equiv of KOH, rt, 30 min, (2) DMF, 1 additional equiv of KOH, rt, TLC monitoring, 45−49%.

values on recombinant *Pf*GSK-3 and on native porcine *Ss*GSK-3 in a radiometric protein kinase assay. The finding that **5u** was inactive on *Pf*GSK-3 confirmed the observation that in series **5** an ortho substituent at the 4-aryl ring is mandatory for *Pf*GSK-3 inhibition. The size of this ortho substituent appears to be important, since large 2-alkoxy substituents (**5a−5h**, **5p**) or the small fluorine substituent (**5cc**) were detrimental for *Pf*GSK-3 inhibitory activity. The halogen substituents iodine, bromine, and chlorine were best suited in the ortho position with a tendency in favor of chlorine. Regarding substitution at the benzoyl ring, all congeners showing submicromolar *Pf*GSK-3 inhibition (**5m**, **5s**, **5v**, **5z**, **5aa**) displayed a substituent in the 3-position, highlighting a preference for this structural pattern. All derivatives of series **5** showing activity on *Pf*GSK-3 were inactive on the mammalian homologue, thus corroborating the direction of selectivity found with hit compound **4**.

The representatives of the small series **6a−6c** deviate from the hit structure **4** by insertion of an additional nitrogen atom between the thieno[2,3-*b*]pyridine and the benzoyl elements. The fact that **6** are completely inactive on *Pf*GSK-3 may originate from a close space limitation of the pocket accommodating the benzoyl substituent. An obvious structural crossover design strategy based on the hit compounds **2** and **4** was realized in series **7** and **8**. When the 2-iodo-substituted 4-aryl substituent and the cyclohexene annulation at the thieno[2,3-*b*]pyridine scaffold were combined, the resulting congeners **8a** and **8b** were found to be completely inactive. A reasonable explanation for this disappointing result would be that **2** and **4** have different binding modes in the enzyme, refuting the rationale for the combination of structure elements. On the other hand, the replacement of the cyclohexene annulation displayed by hit structure **2** with the 6-amino-5-cyano pattern of hit structure **4** led to derivative **7g**, which exhibited marked but unselective *Pf*GSK-3/*Ss*GSK-3 inhibition. A similar unselective GSK-3 inhibitory activity was found with the analogues **7c**, **7d**, and **7f**, which display a comparably small ortho substituent at the phenyl ring. In contrast, **7a**, **7b**, and **7e**, which are distinguished by larger ortho substituents, remained inactive.

For an explanation of the observed structure−activity relationships within the family of thieno[2,3-*b*]pyridines, a comparison of the molecular inhibitor/kinase interactions was desirable. Unfortunately, all attempts to generate crystals of *Pf*GSK-3 in complex with one of the inhibitors of series **5** failed. Therefore, the analogue **7d** showing the highest *Ss*GSK-3 inhibition was cocrystallized with the human enzyme (Figure 1). Hexagonal crystals of the (pTyr216)-GSK3*β*−**7d** complex showed poor diffraction quality. (pTyr216)-GSK3*β* and **7d** were cocrystallized with an axin-derived peptide [axin(383−401)][47] to find a crystal form with better diffraction properties. Crystals of the (pTyr216)-GSK3*β*−axin(383−401)−**7d** complex belonged to the orthorhombic space group $P2_12_12_1$, with one copy of the (pTyr216)-GSK3*β*−axin(383−401)−**7d** complex per crystallographic asymmetric unit.

The crystal structure of the (pTyr216)-GSK3*β*−axin(383−401)−**7d** complex was determined by molecular replacement using the structure of the (pTyr216)-GSK3*β*−axin(383−401) complex[47] as a search model and refined at 2.64 Å resolution. Statistics for data collection and refinement are given in Table 2.

The overall structure of (pTyr216)-GSK3*β*−axin(383−401)−**7d** is basically identical to the (pTyr216)-GSK3*β*−axin(383−401) structure, with the N-terminal lobe of GSK3*β* predom-

Table 2. Crystal Structure Data and Refinement Statistics for GSK-3*β*−7d

space group	$P2_12_12_1$
unit cell params *a*, *b*, *c* (Å)	73.15, 76.16, 86.54
no. of molecules/asu[a]	1
Data Collection (XDS)	
beamline	I02
wavelength (Å)	0.9700
resolution range[b]	45.05−2.64 (2.80−2.64)
no. of observations (unique)	57827 (14488)
completeness (%)	98.8 (97.0)
R_{sym}[c] (%)	6.9 (86.0)
$I/\sigma(I)$	18.0 (2.3)
Refinement (Phenix)	
resolution range (Å)	45.05−2.64
no. reflns in working set	13612
no. of reflns in test set	869
no. of non-hydrogen atoms	3029
no. of solvent water molecules	70
R/R_{free} (%)	20.1/24.2
RMSD(bond length) (Å)	0.003
RMSD(bond angle) (deg)	0.750

[a]asu = asymmetric unit. [b]The values in parentheses of the resolution range, completeness, R_{sym}, and $I/\sigma(I)$ correspond to the outermost resolution shell. [c]$R_{sym} = \sum_{hkl}\sum_j|I(hkl;j) - \langle I(hkl)\rangle|/(\sum_{hkl}\sum_j\langle I(hkl)\rangle)$, where $I(hkl;j)$ is the *j*th measurement of the intensity of the unique reflection (hkl) and $\langle I(hkl)\rangle$ is the mean over all symmetry-related measurements.

dx.doi.org/10.1021/jm301575n | J. Med. Chem. XXXX, XXX, XXX−XXX

inantly consisting of β-sheets and a predominantly α-helical C-terminal lobe (Figure 2A). The axin(383−401) peptide binds as

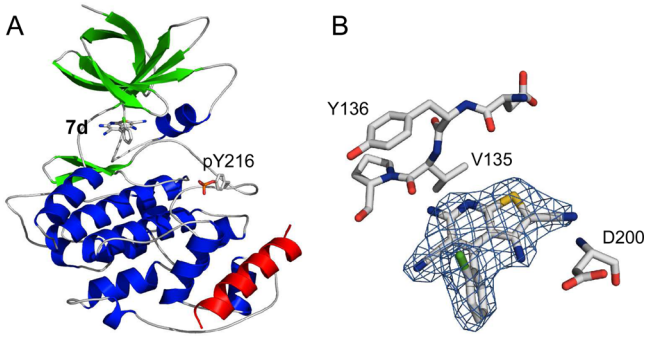

Figure 2. (A) Ribbon diagram showing the overall fold of the (pTyr216)-GSK3β−axin(383−401)−**7d** complex. α-Helices are colored in blue and β-sheets in green. The axin peptide is colored in red. The pTyr216 and **7d** molecules are shown as stick models with atomic colors as follows: oxygen, red; nitrogen, blue; carbon, light gray; sulfur, yellow; chlorine, green. (B) A $2F_o - F_c$ composite annealed omit electron density map of **7d** depicted in chicken wire representation (marine) contoured at 1.0 standard deviation above the mean. Atomic colors are as follows: oxygen, red; nitrogen, blue; carbon, light gray; sulfur, yellow; chlorine, green.

a single amphipathic α-helix into a hydrophobic surface channel on the C-terminal helical domain (Figure 2A). As a prominent difference, the glycine-rich loop (AA62−70) is shifted toward the active site, resulting in a more closed active site conformation. A $2F_o - F_c$ composite annealed omit map shows clear electron density for compound **7d** (Figure 2B).

It was found that **7d** occupies the ATP-binding pocket of the enzyme, representing the characteristic binding mode of small molecular kinase inhibitors to the host protein (Figure 3). Within the pocket, the flat annulated heterocyclic ring system is rendered into position by an ensemble of H-bonds to amino acid residues of the protein. The first H-bond is formed between the inhibitor's 6-amino group and the backbone carbonyl oxygen of Val135, which represents the amino acid three positions downstream of

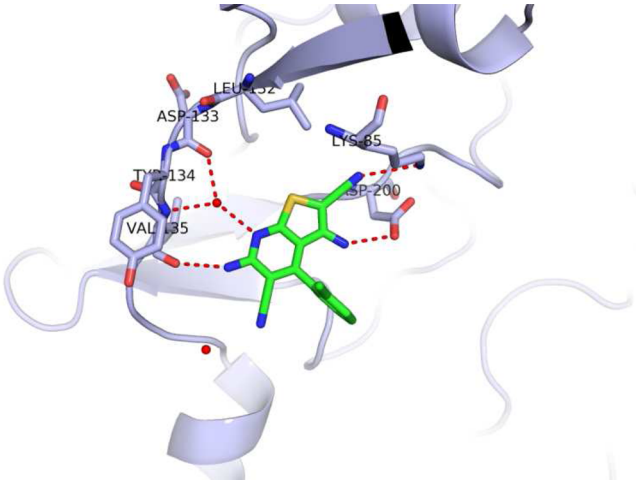

Figure 3. Binding mode of compound **7d** (carbon scaffold shown in green) in *Hs*GSK-3 (X-ray crystal structure). The red spheres correspond to crystallographically observed water molecules, one of which mediates the contact between the ligand and Asp133 (the gk + 1 amino acid). Key binding site residues are depicted as sticks.

the gatekeeper (gk) amino acid. A further hydrogen bond network is mediated by a water molecule located between the inhibitors's pyridine nitrogen atom and the backbone carbonyl oxygen of Asp133 (gk + 1) on one hand and the NH of Val135 on the other hand. Eventually, the 3-amino-2-cyano motif of the ligand shapes a pair of hydrogen bonds directed to the ε-amino group of the conserved Lys85 and to the side chain of Asp200 of the DFG motif. The 4-aryl substituent is oriented orthogonally to the plane of the heterocyclic scaffold, making hydrophobic contacts to Gln185 and Asn186 at the bottom of the ATP-binding pocket (not depicted in Figure 3 for the sake of clarity). The 2-chloro substituent is directed toward the roof of the pocket, where larger substituents (such as iodo or ethoxy) cannot be accommodated, which explains the lack of activity by **7a**, **7b**, and **7e**.

For structure comparison, congener **5v** was docked into the ATP-binding site of a *Pf*GSK-3 homology model[48] we have reported recently and to *Hs*GSK-3 (PDB code 1j1b)[49] using the FlexX module of LeadIT (Figure 4). Docking poses closely

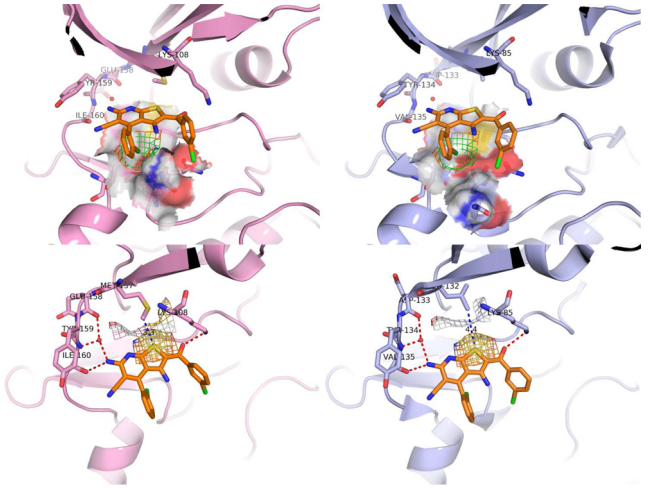

Figure 4. Docking of **5v** (carbon scaffold shown in orange) to *Pf*GSK-3 (left, protein shown in light pink) and *Hs*GSK-3 (right, X-ray crystal structure 1J1B (PDB), protein shown in light blue). Upper row: Illustration of the halogen-binding groove at the bottom of the binding site. The *o*-halogen substituent penetrates the protein surface of the human binding site (right, halogen surface depicted as a mesh), while it fits almost perfectly to the protein surface of the plasmodial enzyme (left). Lower row: Hydrogen-bonding network that anchors the ligand in the binding site. The distance between the heterocyclic sulfur and the respective gatekeeper residue and the hydrophobic contact area are depicted (surface areas of the interacting atoms are shown as meshes). Images were drawn with Pymol 1.4.1 (PyMOL Molecular Graphics System, Schrödinger, LLC).

related to the **7d**−*Hs*GSK-3 complex were generated with **5v** for each target. The 6-amino group of **5v** is making a direct H-bond to the hinge residue Ile160/Val135 and via a water molecule to Glu158/Asp133. The ε-amino group of the conserved Lys 108/Lys85 acts as a hydrogen bond donor to the carbonyl oxygen of the inhibitor **5v**. Both aromatic substituents are perpendicular to the heterocyclic scaffold, but in contrast to the **7d**−*Hs*GSK-3 complex, the ortho substituent of the phenyl ring of **5v** is accommodated in a shallow groove at the bottom of the pocket, which was identified by molecular interaction field calculations as a potential interaction point for halogen substituents in the plasmodial binding site (refer to Figure 4).[34] Due to the bulky 2-aroyl substituent, the heterocyclic plane of **5v** is rotated about

dx.doi.org/10.1021/jm301575n | *J. Med. Chem.* XXXX, XXX, XXX−XXX

30° clockwise and kept in position by a slightly different hydrogen bond network to the hinge residues and the Lys108/85 compared to the position of **7d** in the binding site. In the plasmodial enzyme this leads to a hydrophobic interaction between the gatekeeper side chain (Met157) and the thiophene sulfur of compounds **5**. In the human enzyme such an interaction is not established, because the gatekeeper side chain (Leu132) is located further away from the sulfur atom of ligands **5**. This selectivity phenomenon is not observed with representatives of the **7** series, because these analogues demand less space below the glycine-rich loop and are therefore accommodated equally well in the human and plasmodial enzymes. In contrast, the compounds of the **5** series are much better accommodated in the plasmodial kinase than in the human one. This assumption is supported by the score values for the respective binding poses calculated by the Hyde scoring function. For compound **5v** the value is about 10 kJ/mol higher in the plasmodial enzyme compared to the human one.

The inactive compounds **6** could not be docked to either the plasmodial or the human GSK-3, which is in perfect agreement with our binding mode assumption. Derivatives **8** are inactive because they lack the 6-amino group present in **5**, which is important as a H-bond anchoring group toward the gk + 3 residue of the kinase hinge region.

GSK-3 is a widely conserved enzyme in eukaryotic organisms (Figure 1). It has been pointed out before that selective GSK-3 inhibitors might also be useful to treat infections by other parasites besides *P. falciparum*.[30,35,50,51] Compounds known as or derived from GSK-3 inhibitors have been studied as anti-trypanosomal[51] and antileishmanial[52] agents. In this context, we explored the inhibitory activity of the congeners **4**, **5a, 5m, 5s, 5v**, and **5z** on the GSK-3 homologues of other pathogenic microorganisms belonging to the phylum Apicomplexa, namely, of *Plasmodium knowlesi*, *Toxoplasma gondii*, *Cryptosporidium parvum*, *Trypanosoma cruzi*, *T. brucei*, *Leishmania major*, and *Leishmania donovani*. To further estimate the selectivity of the compounds, we also included the GSK-3 homologues of the slime mold *Dictyostelium discoideum* and the two human GSK-3α and GSK-3β isoforms. The results given in Table 3 show that **4** and **5** indeed selectively inhibit *Pf*GSK-3. The only other parasitic orthologues inhibited by micromolar inhibitor concentrations were GSK-3 of *P. knowlesi*, the closest organism to *P. falciparum*, and GSK-3 of *L. donovani*, the infectious agent causing visceral leishmaniasis (kala azar). The GSK-3 orthologues of the other parasites belonging to the order Trypanosomatida (*L. major*, *T. cruzi*, *T. brucei*) remained unaffected up to 100 μM. The same insensitivity was observed with both GSK-3's of the parasites *T. gondii* and *C. parvum*. Similar to the native porcine enzyme, the recombinant human GSK-3α isoform was not inhibited by congeners **5** listed in Table 3. In contrast, **5s**, **5v**, and **5z** inhibited the human GSK-3β isoform in one-digit micromolar concentrations. Nevertheless, also for these compounds there is still a selectivity gap of 1 order of magnitude for inhibition of the plasmodial and human enzymes. Interestingly, the compounds also inhibited the GSK-3 homologue of another species of *Plasmodium*, *P. knowlesi*. This suggests that the selectivity may extend to GSK-3 orthologues of other *Plasmodium* species, which are also responsible for other forms of malaria, namely, *P. vivax*, *P. ovale*, *P. malariae*, and *P. knowlesi*.

Considering the selectivity data across the GSK-3 orthologues of different species on one hand and overall bioactivity in the compound class on the other hand, we decided to evaluate

Table 3. Inhibition of GSK-3 Orthologues of Different Species by 4 and Selected Congeners 5 (IC_{50}, μM)[a,b]

species	4	5a	5m	5s	5v	5z
Plasmodium falciparum	1.61	6	0.91	0.61	0.48	0.5
Plasmodium knowlesi	15.5	95.0	2.75	1.45	2.45	6.5
Toxoplasma gondii	>100	>100	>100	>100	>100	>100
Cryptosporidium parvum	>100	>100	>100	>100	>100	>100
Trypanosoma cruzi	>100	>100	>100	>100	>100	>100
Trypanosoma brucei	>100	>100	>100	>100	>100	>100
Leishmania major	>100	>100	>100	>100	>100	>100
Leishmania donovani	80	80	70	44	72	100
Dictyostelium discoideum	>100	>100	>100	80	>10	>100
Sus scrofa (GSK-3α/β)	>100	>100	>100	5.6	>10	22
Homo sapiens (GSK-3α)	>100	>100	>100	>100	>100	>25
Homo sapiens (GSK-3β)	>100	>100	50	4.0	3.3	8.1

[a] IC_{50} values were calculated from dose−response curves. The highest inhibitor concentration used in the assays was 10, 25, or 100 μM. [b] All data points were recorded in triplicate. Typically, the standard deviation of the single points was below 10%.

compound **5v** in broad panels of human protein kinases established in the University of Dundee screening platform.[53] Kinase inhibition activity was determined with 1 and 10 μM concentrations of the test compound. None of the 77 kinases was inhibited by the 1 μM compound concentration by more than 50%. The 10 μM concentration of **5v** inhibited only 12 kinases by more than 50% (BRSK2, BTK, CAMK1, CHK2, ERK8, IKKε, IR-HIS, MAPKAP-K2, MKK1, p38α MAPK, P38 β MAPK, PAK4) and only 1 additional kinase (PKB α) by more than 80% (refer to the Supporting Information for details), indicating a high selectivity in favor of *Pf*GSK-3 versus diverse human kinases (Supplementary Table S3).

To complement the selectivity studies, **5v** was screened on the large-scale DiscoverX KinomeScan panel. This interaction assay provides an overall view of the affinity of a compound for any of 402 kinases.[54,55] A semiquantitative scoring of this primary screen was provided (Figure 5). The results showed only low interaction with a few kinases (Figure 5; Supplementary Table S4, Supporting Information).

For evaluation of antiparasitic activity, eight congeners of series **5** showing potent *Pf*GSK-3 inhibition were tested in a luminescence-based assay against erythrocytic stages of *P. falciparum* parasites. For an initial activity assessment, parasites expressing luciferase were incubated for 72 h with a 15 μM concentration of the test compounds and luminescence was measured after cell lysis. Compounds showing more than 80% inhibition of parasite viability were then characterized by determination of EC_{50} values in a similar experiment. The results given in Table 4 show that all test compounds inhibited the parasites at 15 μM. Compounds **5v**, **5w**, **5y**, and **5aa** exhaustively decreased viability at 15 μM and exhibited single-digit micromolar EC_{50} values. Although there is a gap of roughly 1 order of magnitude between concentrations for enzyme inhibition and parasite inhibition, the results demonstrate that *Pf*GSK-3 could serve as an exploitable biological target for the development of antimalarial agents. In terms of structure−activity relationships, the results show that a 2-chloro substituent at the phenyl ring and a halogen-containing substituent at the 3-

dx.doi.org/10.1021/jm301575n | J. Med. Chem. XXXX, XXX, XXX−XXX

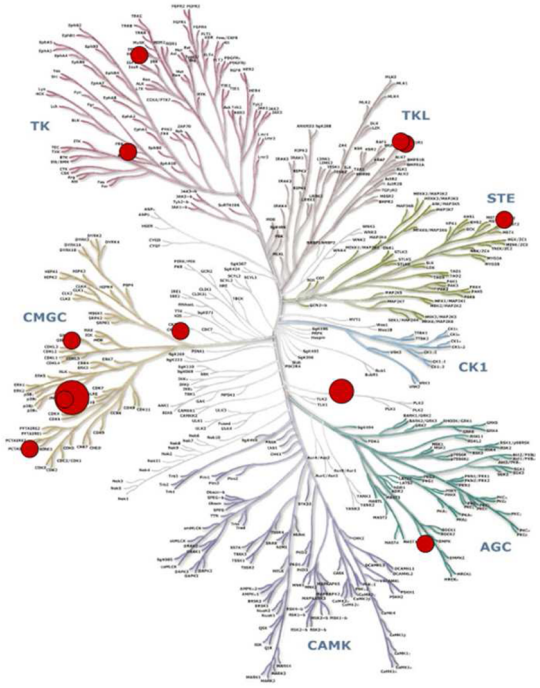

Figure 5. Protein kinase selectivity of compound **5v** tested in a 402 human kinase interaction assay (KinomeScan). Compound **5v** was tested at a 10 μM final concentration in the kinase interaction panel. A semiquantitative scoring of this primary screen was estimated. This score relates to the probability of a hit rather than strict affinity. Scores of >10, between 1 and 10, and <1 indicate the probability of being a false positive, which is <20%, <10%, and <5%, respectively. The results are presented as a TREEspot kinase interaction map (top). Raw data (all 402 values) are provided in the Supporting Information, Table S4.

Table 4. Antiplasmodial Activity of Selected *Pf*GSK-3 Inhibitors

compd	inhibition at 15 μM[a] (%)	EC_{50}[b] (μM)
5m	65.4 (±2.0)	nt
5s	77.1 (±4.6)	nt
5v	100.0 (±0.0)	5.5 (4.2−7.2)
5w	100.0 (±0.0)	3.7 (2.7−5.0)
5x	63.5 (±4.3)	nt
5y	100.0 (±0.0)	5.6 (4.3−7.2)
5z	30.3 (±3.6)	nt
5aa	100.0 (±0.0)	7.5 (4.6−12.3)
control (DMSO)	0.0 (±9.6)	nt

[a]Luminescence assay (luciferase) after 72 h of incubation of *P. falciparum* NF54LUC parasites with compounds at 15 μM. SEM values are given in parentheses. [b]EC_{50} values were determined for compounds showing inhibition rates above 80% and were calculated from dose−response curves. Single data points were measured after 48 h of incubation with test compounds. Confidence intervals are given in parentheses. nt = not tested.

position of the benzoyl ring appear favorable for antiplasmodial activity.

CONCLUSION

We have identified and developed a novel class of selective inhibitors of *Pf*GSK-3, an enzyme that was suggested as a suitable target for antimalarial drugs. Initial hits were identified in an HTS campaign from a commercial compound library. Representatives of the new inhibitor family **5** share the 3,6-diamino-4-(2-halophenyl)-2-benzoylthieno[2,3-*b*]pyridine-5-carbonitrile motif. The compounds of highest potency inhibit *Pf*GSK-3 in submicromolar concentrations and exhibit selectivity versus GSK-3 orthologues of other species and versus other human protein kinases. A structure model providing an informative basis for the *Pf*GSK-3/*Hs*GSK-3 selectivity of **5** was generated by docking studies based on a *Pf*GSK-3 homology model, taking into account the X-ray structure of the related molecule **7d** in complex with human GSK-3. Selected congeners **5** showed in vitro antiplasmodial activity against erythrocyte stages of *P. falciparum* parasites in single-digit micromolar concentrations. The results warrant further development of the structure class toward antimalarial drugs.

EXPERIMENTAL PROCEDURES

Synthetic Chemistry. Starting materials were purchased from the suppliers indicated below and were used without further purification, unless stated otherwise: aromatic aldehydes **9**, cyanothioacetamide (**11**), phenacyl bromides **21**, 2-chloro-*N*-(4-chlorophenyl)acetamide (**22**), and chloroacetonitrile (**23**) were from Acros Organics, Geel, Belgium, and 2-fluorobenzaldehyde and malonodinitrile (**10**) were from Sigma-Aldrich, Steinheim, Germany. Prior to use, liquid aromatic aldehydes **9** (unsubstituted benzaldehyde, 2-chlorobenzaldehyde, 2-bromobenzaldehyde, 2-ethoxybenzaldehyde, 2-methylbenzaldehyde, thiophene-2-carbaldehyde) were purified by extraction with aqueous saturated sodium carbonate solution to remove acidic impurities.

Melting points (mp's) were determined on an electric variable heater (Electrothermal IA 9100) in open glass capillaries. IR spectra were recorded as KBr disks on a Thermo Nicolet FT-IR 200 (remark regarding IR spectra: being part of a vinylogic amide element which may be involved in H-bonding, the carbonyl C═O valence vibration band of compounds **5**, **6**, and **8** is strongly shifted to low wavenumbers and overlaps in most cases the aromatic C═C vibration band). ^{1}H NMR spectra and ^{13}C NMR spectra were recorded on Bruker Avance DRX-400 and Bruker Avance II-600 instruments (NMR Laboratories of the Chemical Institutes of the Technische Universität Braunschweig) with an internal standard of tetramethylsilane, and signals are given in parts per million (δ scale). Elemental analyses were determined on a CE Instruments FlashEA 1112 elemental analyzer (Thermo Quest). Mass spectra were recorded on a Finnigan-MAT 90 double-focused sector field mass spectrometer. Accurate measurements were conducted according to the peakmatch method using perfluorokerosene (PFK) as an internal mass reference. EI-MS: ionization energy 70 eV (Department of Mass Spectrometry of the Chemical Institutes of the Technische Universität Braunschweig). TLC: Polygram Sil G/UV_{254}, Macherey-Nagel, 40 × 80 mm, visualization by UV illumination (254 and 366 nm). Column chromatography: silica gel 60 (Merck), column width 2 cm, column height 10 cm unless stated otherwise. Purity was determined by HPLC using the following devices and settings: Elite LaChrom (Merck/Hitachi), pump L-2130, autosampler L-2200, diode array detector (DAD) L-2450, organizer box L-2000, column Merck LiChroCART 125-4, LiChrosphere 100, RP 18, 5 μm, flow rate 1.000 mL/min, isocratic, volume of injection 10 μL, detection (DAD) at 254 and 280 nm, AUC-%-method; time of detection 15 min, net retention time (t_N), dead time (t_m) related to DMSO. Preparation of H_2O + $(Et_3NH)_2SO_4$ buffer (pH 2.5) for HPLC: Triethylamine (20.0 mL) and sodium hydroxide (242 mg) were dissolved in water (980 mL). The solution was adjusted to pH 2.5 by addition of sulfuric acid. Absorption maxima (λ_{max}) were extracted from the spectra recorded by the DAD in the HPLC peak maxima (software EZ Chrom Elite Client/server version 3.1.3). All compounds employed in biological tests were used in ≥95% purity. Synthetic procedures and structure characterization data for the following compounds are available in the Supporting Information: **12**−**16**, **18**−**20**, **5a**−**5u**, **5w**−**5cc**, **6a**−**6c**, **7a**−**7h**, **8a**, **8b**.

*General Procedure A for the Preparation of 6-Amino-4-aryl-2-thioxo-1,2-dihydropyridine-3,5-dicarbonitriles **12**−**20**.* A suitable aromatic aldehyde, **9** (1.00 mmol), malonodinitrile (**10**; 1.00 mmol), and cyanothioacetamide (**11**; 1.00 mmol) were dissolved in EtOH (4

dx.doi.org/10.1021/jm301575n | J. Med. Chem. XXXX, XXX, XXX−XXX

mL). Piperidine (50 μL) was added, and the mixture was refluxed for 3 h. After evaporation of the solvent in vacuo, glacial acetic acid (six drops), water (10 mL), and CH_2Cl_2 (2 mL) were added, and the mixture was shaken for 1 min. A precipitate was formed either immediately or after storage overnight at 2−5 °C. The precipitate was filtered off with suction and used for the following synthetic steps without further purification.

*6-Amino-4-(2-chlorophenyl)-2-thioxo-1,2-dihydropyridine-3,5-dicarbonitrile (**17**).* Preparation according to general procedure A from 2-chlorobenzaldehyde, **10**, and **11** yielded a yellow powder (57%). Mp: 177−180 °C (lit.[56] 180−182 °C).

*General Procedure B for the Synthesis of 3,6-Diamino-2-aroyl-4-arylthieno[2,3-b]pyridine-5-carbonitriles **5**, 3,6-Diamino-4-aryl-N-(4-chlorophenyl)-5-cyanothieno[2,3-b]pyridine-2-carboxamides **6**, 3,6-Diamino-4-arylthieno[2,3-b]pyridine-2,5-dicarbonitriles **7**, and (3-Amino-4-aryl-5,6,7,8-tetrahydrothieno[2,3-b]quinolin-2-yl)(aryl)-methanones **8**.* A suitable precursor compound, **12**−**20** or **26** (0.400 mmol), was dissolved in DMF (0.5 mL). After addition of 10% aqueous KOH (224 μL), the mixture was stirred for 1 min. A suitable haloalkane, **21**, **22**, or **23** (0.400 mmol), was added, and stirring was continued for 30 min at room temperature. After addition of a second portion of 10% aqueous KOH (224 μL), stirring was continued at room temperature. The reaction was monitored by TLC. Completion of the reaction was detected after the reaction time specified in the distinct procedure descriptions. Upon addition of water (5 mL), a precipitate formed which was filtered off with suction and washed successively with water, EtOH, and petroleum ether. Purification was accomplished by column chromatography or crystallization from the indicated solvents.

*3,6-Diamino-2-(3-chlorobenzoyl)-4-(2-chlorophenyl)thieno[2,3-b]pyridine-5-carbonitrile (**5v**).* Preparation was according to general procedure B from **17** and 2-bromo-1-(3-chlorophenyl)ethanone, reaction time 3.5 h. Crystallization from EtOH yielded an orange powder (37%). Mp: 289−290 °C. IR (KBr): 3477 and 3362 cm^{-1} (NH), 2216 cm^{-1} (C≡N). ^1H NMR (DMSO-d_6, 600 MHz): δ (ppm) = 6.69 (br s, 2 H, NH_2), 7.54−7.56 (m, 1 H, ArH), 7.62−7.64 (m, 1 H, ArH), 7.65−7.67 (m, 4 H, ArH), 7.69−7.72 (m, 1 H, ArH), 7.76−7.91 (m, 3 H, NH_2 and ArH overlapping). ^{13}C NMR (DMSO-d_6, 150.9 MHz): δ (ppm) = 125.7, 126.9, 128.6, 130.0, 130.4, 130.6, 130.8, 132.5 (tertiary C); 90.9, 99.6, 112.4, 114.8, 131.1, 131.8, 133.4, 142.7, 150.8, 151.2, 159.3, 166.4, 185.9 (quaternary C). Anal. ($C_{21}H_{12}Cl_2N_4OS$) C, H, N, S. HPLC: 98.0% at 254 nm and 98.0% at 280 nm, t_N = 5.39 min, t_M = 1.03 min (ACN/H_2O, 55:45), λ_{max} = 328 nm.

Kinase Expression and Activity Assays. *GSK-3 Orthologue Clones.* The *Pk*GSK3 (*P. knowlesi* GSK3) gene was synthezised by GenCust and cloned into the expression vector plasmid pBAD-Thio-TOPO (Invitrogen).

The *Tg*GSK3 (*To. gondii* GSK3) gene was generated by PCR from *To. gondii* cDNA using a 5′-primer, ATGCCGGACCCGCAGTACGA-TCC (F-Toxog), and a 3′-primer, GCCACGGTTGTTTGCACTGG-CG (R-Toxog), and provided by Maryse Lebrun (Jean-François Dubremetz laboratory, Montpellier, France). The gene was cloned into the expression vector pBAD-Thio-TOPO (Invitrogen) by direct insertion of the Taq polymerase amplified PCR product.

The *Cp*GSK3 (*C. parvum* GSK3) gene, kindly provided by Dr. Raymond Hui (Structural Genomics Consortium, Toronto, Canada), was cloned into the expression vector pET15-MHL.

GSK-3 orthologues from *T. cruzi* and *T. brucei* were kindly tested by Dr. Wesley C. Van Voohis (Department of Medicine, University of Washington, Seattle, WA).

GSK-3 orthologues from *L. major* and *L. donovani* were kindly tested by Dr. Evangelia Xingi (Pasteur Institute, Athens, Greece).

D. discoideum GSK-3 was kindly provided by Dr. Adrian J. Harwood and Dr. W. Jonathan Ryves (Cardiff School of Biosciences, Cardiff University, Cardiff, U.K.).

Nt-GST-tagged human GSK-3α and GSK-3β were obtained from BPS Bioscience.

Expression of Recombinant (His)$_6$-Tagged Pf GSK3, PkGSK3, TgGSK3, and CpGSK3. Recombinant proteins were expressed in *Escherichia coli* as previously described.[27] Recombinant *E. coli* TOP10 containing expression plasmids pBAD-Thio-TOPO *Pf*GSK3, *Pk*GSK3, and *Tg*GSK3 were streaked on an LB (Luria−Bertani) broth plate in the presence of ampicillin (100 μg/mL). A single colony was inoculated into 5 mL of LB medium (tryptone, 10 g/L; yeast extract, 5 g/L; NaCl, 10 g/L; pH 7.5) with ampicillin (100 μg/mL) and incubated at 37 °C overnight. The culture was then transferred into 250 mL of LB medium with ampicillin (100 μg/mL) in a 1 L bottle and cultured at 37 °C under constant shaking (250 rpm) to an OD_{600} of ∼0.5. Expression was induced with 0.5 mL of 20% arabinose (0.02% final concentration) for 4 h at 37 °C under constant shaking.

Recombinant *E. coli* BL21-(DE3)-pRARE2 containing expression plasmid pET15-MHL *Cp*GSK3 was streaked on an LB broth plate in the presence of ampicillin/chloramphenicol (100 and 34 μg/mL). A single colony was inoculated into 5 mL of LB medium with ampicillin/chloramphenicol (100 and 34 μg/mL, respectively) and incubated at 37 °C overnight. Then the culture was transferred into 250 mL of LB medium with ampicillin/chloramphenicol (100 and 34 μg/mL, respectively) in a 1 L bottle, cultured at 37 °C under shaking (250 rpm) to an OD_{600} of ∼0.5, cooled to 15 °C, and induced with 0.5 mM isopropyl 1-thio-D-galactopyranoside overnight at 15 °C under constant shaking.

Cultures were harvested by centrifugation at 9000 rpm for 10 min. Bacterial pellets were stored at −80 °C.

Extraction and Purification of Recombinant (His)$_6$-Tagged Pf GSK3, PkGSK3, TgGSK3, and CpGSK3 and Purification of Mammalian GSK-3. Extraction. Pellets from 250 mL *E. coli* cultures were resuspended to approximately 10 mL in lysis buffer (50 mM HEPES, pH 7.5, 500 mM NaCl, 5 mM imidazole, and 5% glycerol) with the addition of protease inhibitors (Complete EDTA-free inhibitor cocktail from Roche). Resuspended pellets stored at −80 °C were thawed overnight at 4 °C the day before purification. Prior to lysis, each pellet from a 250 mL culture was pretreated with lysozyme, 300 μg/mL final (or 0.5% CHAPS), and 500 units of DNase I for 30 min at room temperature. Cells were disrupted by potterization and sonication, and the cell lysate was centrifuged at 24 000 rpm for 30 min at 4 °C.

Purification. Recombinant *Pf*GSK3, *Pk*GSK3, *Tg*GSK3, and *Cp*GSK3 proteins were purified by immobilized metal affinity chromatography by a batch procedure on 500 μL (for 10 mL of lysate) of nickel affinity resin (Ni−NTA (nitrilotriacetic acid) agarose beads, Qiagen). The beads were washed four times with 10 mL of washing buffer (50 mM HEPES, pH 7.5, 500 mM NaCl, 30 mM imidazole, 5% glycerol). The lysates were incubated with the beads for 2 h at 4 °C on a rotating wheel. After centrifugation (1500 rpm, 2 min at 4 °C) the beads were washed four times with 1 volume of wash buffer. Proteins were then eluted successively three times with respectively 500 μL (first elution), 300 μL (second elution), and 200 μL (third elution) of elution buffer (50 mM HEPES, pH 7.5, 500 mM NaCl, 250 mM imidazole, 5% glycerol). The protein identity and purity were evaluated by SDS−PAGE analysis. Samples were stored at −80 °C.

Mammalian GSK-3. GSK-3α/β was purified from porcine brain by affinity chromatography on immobilized axin.[57]

Kinase Assays. The activity of the recombinant kinases was measured by incubating the proteins with 40 μM GS-1 peptide substrate (YRRAAVPPSPSLSRHSSPHQpSEDEEE, where pS stands for phosphorylated serine; Proteogenix, Oberhausbergen, France) in buffer A, pH 7.5 (10 mM $MgCl_2$, 1 mM EGTA, 1 mM DTT, 25 mM Tris/HCl, pH 7.5, 50 μg/mL heparin, 0.15 mg/mL BSA), in the presence of 15 μM γ-^{33}P-ATP in a final volume of 30 μL. After 30 min of incubation at 30 °C except for *Dd*GSK3 (30 min at room temperature), 25 μL of the reaction was spotted onto Whatman P81 phosphocellulose paper. The filters were washed five times (for at least 5 min each time) in a 1% phosphoric acid solution. The wet filters were counted in the presence of 1 mL of ACS (Amersham) scintillation fluid. Blank values were subtracted and activities calculated as picomoles of phosphate incorporated during a 30 min incubation. The activities are usually expressed as a percentage of the maximal activity, i.e., in the absence of inhibitors. Controls were performed with appropriate dilutions of dimethyl sulfoxide. For molecules showing inhibitory activity at 10 μM, dose−response curves were performed to calculate the IC_{50} value.

Compound Libraries. The compound library for high-throughput screening was obtained through the WHO. It comprised compounds from ChemDiv (5000 kinase inhibitory scaffolds plus a collection of 5000 random compounds) and Biospecs (480 products). The focused

library was supplied by ChemDiv. It comprised 427 compounds containing the thieno[2,3-*b*]pyridine parent scaffold.

Crystallography and Molecular Modeling. *GSK-3 Crystal Structures.* The human (pTyr216)-GSK3β–axin(383–401) complex was prepared as previously described.[47] Samples of the (pTyr216)-GSK3β–axin(383–401) complex [6 mg/mL GSK3b + 0.37 mg/mL axin(383–401)] were incubated on ice with 500 μM **7d** for 1 h prior to crystallization.

Crystals of the (pTyr216)-GSK3β–axin(383–401)–**7d** complex were obtained within 6 weeks by the hanging drop vapor diffusion method mixing 1 μL of complex with 1 μL of reservoir solution containing 0.1 M 2-(*N*-morpholino)ethanesulfonic acid (MES), pH 6.5, and 12% (w/v) PEG 20 000 at 20 °C. Crystals belong to the orthorhombic space group $P2_12_12_1$ with cell dimensions of a = 73.15 Å, b = 76.16 Å, and c = 86.54 Å and one copy of the (pTyr216)-GSK3β–axin(383–401)–**7d** complex per crystallographic asymmetric unit.

X-ray data were collected at beamline I02 at the Diamond Light Source (Oxfordshire, U.K.) using an ADSC Quantum Q315r detector. Processing was performed using the program XDS.[58]

The structure was solved by molecular replacement with the program PHASER[59] employing the (pTyr216)-GSK3β–axin(383–401) complex[47] (PDB code 1O9U) as a search model. Bound ligand in the active site was identified by the difference Fourier method. Structure refinement and model building were performed using iterative cycles of phenix.refine[60] and Coot.[61] Crystallographic statistics are given in Table 2. The coordinates were deposited in the RCSB Protein Data Bank[62] with accession number 3ZDI. $2F_o - F_c$ composite annealed omit electron density maps were calculated with CNS.[63] Figures were prepared with PyMOL (www.pymol.org).

Docking. Docking studies were accomplished by the FlexX module of LeadIT 2.0.2 (BiosolveIT GmbH, St. Augustin, Germany, 2011). Receptors were prepared by the standard setup routine using the 1J1B PDB file[49] for the human enzyme and a corresponding *Pf*GSK-3 model.[48] Basic and acidic binding site side chains were protonated or deprotonated, respectively. Two water molecules observed in the X-ray structure of **7d** were merged into the binding sites and defined as freely rotatable and displaceable during the docking procedure. Ligands were constructed with SYBYL X1.3 and minimized using AM1 charges and the Tripos force field. The single interaction scan (SIS) mode of FlexX[64–67] was used for base fragment placement, and the obtained poses were rescored by the new Hyde scoring function.[68]

in Vitro Antimalarial Activity Assay. Erythrocytic stages of *P. falciparum* parasites stably expressing the luciferase gene by the *hrp2* promoter from a chromosomal locus (NF54:*LUC*) were used. These parasites constitutively express high levels of luciferase. Cultures of 20 mL total volume were grown in 75 mL tissue culture flasks (Costar brand, NUNC, Denmark) as previously described.[69] Upon reaching 3% parasitemia, the medium was aspirated and 100 μL of 25% hematocrit cultured parasites was transferred with a multichannel pipet to a 96-well sterile plate (100 μL in each well). Drugs diluted in complete RPMI-1640 containing 1% DMSO (10 μM, 100 μL/well) were added to each well. Each drug was tested in triplicate. As controls three wells of (NF54:*LUC*) in regular medium with no drug and another three wells in which (NF54:*LUC*) is exposed only to the 1% DMSO were inoculated. Three additional wells were inoculated with NF54 "wild-type" parasites that do not express luciferase and were used as "blanks". The plate was incubated in a sealed culture chamber and incubated for 48 h (37 °C, 90% N_2, 5% CO_2, and 5% O_2). After 48 h, 100 μL of the medium was removed and the red blood cells were lysed with the addition of lysis buffer of the Bright-Glo luciferase assay system (100 μL/well, Promega, MT) and incubation at room temperature for 5 min. A 100 μL volume was transferred into an opaque 96-well flat-bottom plate (Costar brand, NUNC, Denmark) for the luciferase assay, and the rest was frozen at −20 °C. A 100 μL volume of the Bright-Glo substrate was added to each well, and the luminescence was measured after 5 min using a microplate reader (Fluoroskan Ascent, Thermo Labsystems, Finland). After screening the activity of the compounds at 15 μM, titrations were carried out to determine the IC_{50} of the most active compounds as described above.

■ ASSOCIATED CONTENT

Ⓢ Supporting Information

*Pf*GSK-3 and GSK-3α/β sensitivity to a panel of kinase inhibitors (Biomol, Supplementary Table S1), accession codes of GSK-3 orthologues used in this study (Supplementary Table S2), results of kinase inhibition by **5v** in the University of Dundee kinase selectivity panel (77 kinases, Supplementary Table S3), results of kinase inhibition by **5v** in the DiscoveRx kinase selectivity panel (402 kinases, Supplementary Table S4), details for the synthesis and spectroscopic data of compounds **12**–**16**, **18**–**20**, **5a**–**5u**, **5w**–**5cc**, **6a**–**6c**, **7a**–**7h**, **8a**, and **8b**, and HPLC purity data of all compounds employed in biological tests. This material is available free of charge via the Internet at http://pubs.acs.org.

■ AUTHOR INFORMATION

Corresponding Author

*E-mail: meijer@manros-therapeutics.com (L.M.); c.kunick@tu-braunschweig.de (C.K.). Phone: +33-608605834 (L.M.); +49-5313912754 (C.K.). Fax: +33-298725528 (L.M.); +49-5313912799 (C.K.).

Notes

The authors declare no competing financial interest.

■ ACKNOWLEDGMENTS

This work was funded in part by the Commission of the European Communities (Contracts LSHB-CT-2004-503467 and Health-F3-2008-223414 to L.M. and C.K., FP7 HEALTH-2007-2.3.4-1 LEISHDRUG to L.M., and HEALTH, LSH-2003-2.3.0_2 ANTIMAL to L.M.). This joint project was financially supported by the State of Lower-Saxony, Hannover, Germany (to R.D., N.P., and C.K). S.K. was supported by a Ph.D. grant from the University of Hamburg, Germany. We are thankful to Evangelia Xingi for performing the *Leishmania* GSK-3 assays, to Wesley C. Van Voohis for assaying the *Trypanosoma* GSK-3, to Maryse Lebrun and Jean-François Dubremetz for providing the *Tg*GSK-3 cDNA, to Adrian J. Harwood and W. Jonathan Ryves for providing *Dd*GSK-3, and to Raymond Hui for the *Cp*GSK-3 cDNA.

■ ABBREVIATIONS USED

ACN, acetonitrile; DAD, diode array detector; DFG, aspartate–phenylalanine–glycine sequence; EGTA, ethylene glycol tetraacetic acid; EWG, electron-withdrawing group; gk, gatekeeper; GSK-3, glycogen synthase kinase-3; HEPES, *N*-(2-hydroxyethyl)piperazine-*N*′-2-ethanesulfonic acid; LB, Luria–Bertani; MES, 2-(*N*-morpholino)ethanesulfonic acid; *Pf*CDPK1, *Plasmodium falciparum* calcium-dependent protein kinase 1; PFK, perfluorokerosene; *Pf*mrk, *Plasmodium falciparum* MO15-related protein kinase; *Pf*nek-1, *Plasmodium falciparum* NIMA-related protein kinase; *Pf*PK7, *Plasmodium falciparum* protein kinase 7; RPMI, Roswell Park Memorial Institute

■ REFERENCES

(1) WHO World Malaria Report 2010. http://www.who.int/malaria/world_malaria_report_2010/worldmalariareport2010.pdf (accessed June 8, 2011).

(2) Schlitzer, M. Malaria chemotherapeutics part I: History of antimalarial drug development, currently used therapeutics, and drugs in clinical development. *ChemMedChem* **2007**, *2*, 944–986.

(3) Schlitzer, M. Antimalarial drugs—What is in use and what is in the pipeline. *Arch. Pharm. Chem. Life Sci.* **2008**, *341*, 149–163.

(4) Fidock, D. A. Priming the antimalaria pipeline. *Nature* **2010**, *465*, 297−298.
(5) Gamo, F. J.; Sanz, L. M.; Vidal, J.; de Cozar, C.; Alvarez, E.; Lavandera, J. L.; Vanderwall, D. E.; Green, D. V.; Kumar, V.; Hasan, S.; Brown, J. R.; Peishoff, C. E.; Cardon, L. R.; Garcia-Bustos, J. F. Thousands of chemical starting points for antimalarial lead identification. *Nature* **2010**, *465*, 305−310.
(6) Schlitzer, M.; Ortmann, R. Feeding the antimalarial pipeline. *ChemMedChem* **2010**, *5*, 1837−1840.
(7) Canduri, F.; Perez, P. C.; Caceres, R. A.; de Azevedo, W. F. J. Protein kinases as targets for antiparasitic chemotherapy drugs. *Curr. Drug Targets* **2007**, *8*, 389−398.
(8) Doerig, C. Protein kinases as targets for anti-parasitic chemotherapy. *Biochim. Biophys. Acta* **2004**, *1697*, 155−168.
(9) Doerig, C.; Meijer, L. Antimalarial drug discovery: Targeting protein kinases. *Expert Opin. Ther. Targets* **2007**, *11*, 279−290.
(10) Doerig, C.; Meijer, L.; Mottram, J. C. Protein kinases as drug targets in parasitic protozoa. *Trends Parasitol.* **2002**, *18*, 366−371.
(11) Lawton, P.; Sarciron, M.-É.; Pétavy, A.-F. Chemotherapeutic targets for antiparasitic therapy. *Drugs Future* **2007**, *31*, 793−809.
(12) Jirage, D.; Keenan, S. M.; Waters, N. C. Exploring novel targets for antimalarial drug discovery: Plasmodial protein kinases. *Infect. Disord.: Drug Targets* **2010**, *10*, 134−146.
(13) Doerig, C.; Billker, O.; Haystead, T.; Sharma, P.; Tobin, A. B.; Waters, N. C. Protein kinases of malaria parasites: An update. *Trends Parasitol.* **2008**, *24*, 570−577.
(14) Ward, P.; Equinet, L.; Packer, J.; Doerig, C. Protein kinases of the human malaria parasite *Plasmodium falciparum*: The kinome of a divergent eukaryote. *BMC Genomics* **2004**, *5*, 19.
(15) Doerig, C.; Abdi, A.; Bland, N.; Eschenlauer, S.; Dorin-Semblat, D.; Fennell, C.; Halbert, J.; Holland, Z.; Nivez, M.-P.; Semblat, J.-P.; Sicard, A.; Reininger, L. Malaria: Targeting parasite and host cell kinomes. *Biochim. Biophys. Acta* **2010**, *1804*, 604−612.
(16) Dorin, D.; Le Roch, K.; Sallicandro, P.; Alano, P.; Parzy, D.; Poullet, P.; Meijer, L.; Doerig, C. Pfnek-1, a NIMA-related kinase from the human malaria parasite *Plasmodium falciparum*. *Eur. J. Biochem.* **2001**, *268*, 2600−2608.
(17) Laurent, D.; Jullian, V.; Parenty, A.; Knibiehler, M.; Dorin, D.; Schmitt, S.; Lozach, O.; Lebouvier, N.; Frostin, M.; Alby, F.; Maurel, S.; Doerig, C.; Meijer, L.; Sauvain, M. Antimalarial potential of xestoquinone, a protein kinase inhibitor from a Vanuatu marine sponge *Xestospongia* sp. *Bioorg. Med. Chem.* **2006**, *14*, 4477−4482.
(18) Bouloc, N.; Large, J. M.; Smiljanic, E.; Whalley, D.; Ansell, K. H.; Edlin, C. D.; Bryans, J. S. Synthesis and in vitro evaluation of imidazopyridazines as novel inhibitors of the malarial kinase PfPK7. *Bioorg. Med. Chem. Lett.* **2008**, *18*, 5294−5298.
(19) Merckx, A.; Echalier, A.; Langford, K.; Sicard, A.; Langsley, G. Structures of *P. falciparum* protein kinase 7 identify an activation motif and leads for inhibitor design. *Structure* **2008**, *16*, 228−238.
(20) Geyer, J. A.; Keenan, S. M.; Woodard, C. L.; Thompson, P. A.; Gerena, L.; Nichols, D. A.; Gutteridge, C. E.; Waters, N. C. Selective inhibition of Pfmrk, a *Plasmodium falciparum* CDK by antimalarial 1,3-diaryl-2-propenones. *Bioorg. Med. Chem. Lett.* **2009**, *19*, 1982−1985.
(21) Woodard, C. L.; Li, Z.; Kathcart, A. K.; Terrell, J.; Gerena, L.; Lopez-Sanchez, M.; Kyle, D. E.; Bhattacharjee, A. K.; Nichols, D. A.; Ellis, W.; Prigge, S. T.; Geyer, J. A.; Waters, N. C. Oxindole-based compounds are selective inhibitors of *Plasmodium falciparum* cyclin dependent protein kinases. *J. Med. Chem.* **2003**, *46*, 3877−3882.
(22) Xiao, Z.; Waters, N. C.; Woodard, C. L.; Li, Z.; Li, P.-K. Design and synthesis of Pfmrk inhibitors as potential antimalarial agents. *Bioorg. Med. Chem. Lett.* **2001**, *11*, 2875−2878.
(23) Keenan, S. M.; Geyer, J. A.; Welsh, W. J.; Prigge, S. T.; Waters, N. C. Rational inhibitor design and iterative screening in the identification of selective plasmodial cyclin dependent kinase inhibitors. *Comb. Chem. High Throughput Screening* **2005**, *8*, 27−38.
(24) Woodard, C. L.; Keenan, S. M.; Gerena, L.; Welsh, W. J.; Geyer, J. A.; Waters, N. C. Evaluation of broad spectrum protein kinase inhibitors to probe the architecture of the malarial cyclin dependent protein kinase Pfmrk. *Bioorg. Med. Chem. Lett.* **2007**, *17*, 4961−4966.
(25) Caridha, D.; Kathcart, A. K.; Jirage, D.; Waters, N. C. Activity of substituted thiophene sulfonamides against malarial and mammalian cyclin dependent protein kinases. *Bioorg. Med. Chem. Lett.* **2010**, *20*, 3863−3867.
(26) Lemercier, G.; Fernandez-Montalvan, A.; Shaw, J. P.; Kugelstadt, D.; Bomke, J.; Domostoj, M.; Schwarz, M. K.; Scheer, A.; Kappes, B.; Leroy, D. Identification and characterization of novel small molecules as potent inhibitors of the plasmodial calcium-dependent protein kinase. *Biochemistry* **2009**, *48*, 6379−6389.
(27) Droucheau, E.; Primot, A.; Thomas, V.; Mattei, D.; Knockaert, M.; Richardson, C.; Sallicandro, P.; Alano, P.; Jafarshad, A.; Baratte, B.; Kunick, C.; Parzy, D.; Pearl, L.; Doerig, C.; Meijer, L. *Plasmodium falciparum* glycogen synthase kinase-3: Molecular model, expression, intracellular localisation and selective inhibitors. *Biochim. Biophys. Acta* **2004**, *1697*, 181−196.
(28) Solyakov, L.; Halbert, J.; Alam, M. M.; Semblat, J. P.; Dorin-Semblat, D.; Reininger, L.; Bottrill, A. R.; Mistry, S.; Abdi, A.; Fennell, C.; Holland, Z.; Demarta, C.; Bouza, Y.; Sicard, A.; Nivez, M. P.; Eschenlauer, S.; Lama, T.; Thomas, D. C.; Sharma, P.; Agarwal, S.; Kern, S.; Pradel, G.; Graciotti, M.; Tobin, A. B.; Doerig, C. Global kinomic and phospho-proteomic analyses of the human malaria parasite *Plasmodium falciparum*. *Nat. Commun.* **2011**, *2*, 565.
(29) Zakaria, N. A.; Embi, N.; Sidek, H. M. Suppression of *Plasmodium berghei* parasitemia by LiCl in an animal infection model. *Trop. Biomed.* **2010**, *27*, 624−631.
(30) Oduor, R. O.; Ojo, K. K.; Williams, G. P.; Bertelli, F.; Mills, J.; Maes, L.; Pryde, D. C.; Parkinson, T.; Van Voorhis, W. C.; Holler, T. P. *Trypanosoma brucei* glycogen synthase kinase-3, a target for anti-trypanosomal drug development: A public-private partnership to identify novel leads. *PLoS Neglected Trop. Dis.* **2011**, *5*, e1017.
(31) Pies, T.; Schaper, K.-J.; Leost, M.; Zaharevitz, D. W.; Gussio, R.; Meijer, L.; Kunick, C. CDK1-inhibitory activity of paullones depends on electronic properties of 9-substituents. *Arch. Pharm. (Weinheim, Ger.)* **2004**, *337*, 486−492.
(32) Wieking, K.; Knockaert, M.; Leost, M.; Zaharevitz, D. W.; Meijer, L.; Kunick, C. Synthesis of paullones with aminoalkyl side chains. *Arch. Pharm. (Weinheim, Ger.)* **2002**, *335*, 311−317.
(33) Xie, X.; Lemcke, T.; Gussio, R.; Zaharevitz, D. W.; Leost, M.; Meijer, L.; Kunick, C. Epoxide-containing side chains enhance antiproliferative activity of paullones. *Eur. J. Med. Chem.* **2005**, *40*, 655−661.
(34) Kruggel, S.; Lemcke, T. Comparative investigation of the ATP-binding site of human and plasmodial glycogen synthase kinase-3. *QSAR Comb. Sci.* **2009**, *28*, 885−890.
(35) Osolodkin, D. I.; Zakharevich, N. V.; Palyulin, V. A.; Danilenko, V. N.; Zefirov, N. S. Bioinformatic analysis of glycogen synthase kinase 3: Human versus parasite kinases. *Parasitology* **2011**, *138*, 725−735.
(36) Chen, C.; Mackey, A. J.; Stoeckert, J., C. J.; Roos, D. S. OrthoMCL-DB: Querying a comprehensive multi-species collection of ortholog groups. *Nucleic Acids Res.* **2006**, *34* (Suppl. 1), D363−368.
(37) Thompson, J. D.; Higgins, D. G.; Gibson, T. J. CLUSTAL W: Improving the sensitivity of progressive multiple sequence alignment through sequence weighting, position-specific gap penalties and weight matrix choice. *Nucleic Acids Res.* **1994**, *22*, 4673−4680.
(38) Guindon, S.; Dufayard, J. F.; Lefort, V.; Anisimova, M.; Hordijk, W.; Gascuel, O. New algorithms and methods to estimate maximum-likelihood phylogenies: Assessing the performance of PhyML 3.0. *Syst. Biol.* **2010**, *59*, 307−321.
(39) Guindon, S.; Gascuel, O. A simple, fast and accurate algorithm to estimate large phylogenies by maximum likelihood. *Syst. Biol.* **2003**, *52*, 696−704.
(40) Le, S. Q.; Gascuel, O. An improved general amino acid replacement matrix. *Mol. Biol. Evol.* **2008**, *25*, 1307−1320.
(41) Sharanin, Y. A.; Krivokolysko, S. G.; Dyachenko, V. D. Cyclization reactions of nitriles. LIV. Synthesis and properties of 6-amino-4-aryl-3,5-dicyanopyridin-2(1H)-ones, the corresponding thiones, the pyridylidenemalononitriles and their hydrogenated analogs. *Russ. J. Org. Chem.* **1994**, *30*, 620−626.

(42) Sharanin, Y. A.; Shestopalov, A. M.; Litvinov, V. P.; Klokol, G. V.; Mortikov, V. Y.; Demerkov, A. S. Cyclization reactions of nitriles. XV. Synthesis and reactions of chalcogen-containing 6-amino-3,5-dicyanopyridines. *Russ. J. Org. Chem.* **1988**, *24*, 771−776.
(43) Granik, V. G.; Kadushkin, A. V.; Liebscher, J. Synthesis of amino derivatives of five-membered heterocycles by Thorpe-Ziegler cyclization. *Adv. Heterocycl. Chem.* **1998**, *72*, 79−125.
(44) Litvinov, V.; Dotsenko, V.; Krivokolysko, S. The chemistry of thienopyridines. *Adv. Heterocycl. Chem.* **2007**, *93*, 117−178.
(45) Litvinov, V. P.; Dotsenko, V. V.; Krivokolysko, S. G. Thienopyridines: Synthesis, properties, and biological activity. *Russ. Chem. Bull., Int. Ed.* **2005**, *54*, 864−904.
(46) Elnagdi, M. H.; Abdelrazek, F. M.; Ibrahim, N. S.; Erian, A. W. Studies on alkyl heteroaromatic compounds. The reactivity of alkyl polyfunctionally substituted azines towards electrophilic reagents. *Tetrahedron* **1989**, *45*, 3597−3604.
(47) Dajani, R.; Fraser, E.; Roe, S. M.; Yeo, M.; Good, V. M.; Thompson, V.; Dale, T. C.; Pearl, L. H. Structural basis for recruitment of glycogen synthase kinase 3β to the axin-APC scaffold complex. *EMBO J.* **2003**, *22*, 494−501.
(48) Kruggel, S.; Lemcke, T. Generation and evaluation of a homology model of PfGSK-3. *Arch. Pharm. Chem. Life Sci.* **2009**, *342*, 327−332.
(49) Aoki, M.; Yokota, T.; Sugiura, I.; Sasaki, C.; Hasegawa, T.; Okumura, C.; Ishiguro, K.; Kohno, T.; Sugio, S.; Matsuzaki, T. Structural insight into nucleotide recognition in tau-protein kinase I/glycogen synthase kinase 3 β. *Acta Crystallogr.* **2004**, *D60*, 439−446.
(50) Ojo, K.; Arakaki, T.; Napuli, A.; Inampudi, K.; Keyloun, K.; Zhang, L.; Hol, W.; Verlinde, C.; Merritt, E.; Van Voorhis, W. Structure determination of glycogen synthase kinase-3 from *Leishmania major* and comparative inhibitor structure-activity relationships with *Trypanosoma brucei* GSK-3. *Mol. Biochem. Parasitol.* **2011**, *176*, 98−108.
(51) Ojo, K. K.; Gillespie, J. R.; Riechers, A. J.; Napuli, A. J.; Verlinde, C. L.; Buckner, F. S.; Gelb, M. H.; Domostoj, M. M.; Wells, S. J.; Scheer, A.; Wells, T. N.; Van Voorhis, W. C. Glycogen synthase kinase 3 is a potential drug target for African trypanosomiasis therapy. *Antimicrob. Agents Chemother.* **2008**, *52*, 3710−3717.
(52) Reichwald, C.; Shimony, O.; Dunkel, U.; Sacerdoti-Sierra, N.; Jaffe, C. L.; Kunick, C. 2-(3-Aryl-3-oxopropen-1-yl)-9-*tert*-butylpaullones: A new antileishmanial chemotype. *J. Med. Chem.* **2008**, *51*, 659−665.
(53) Bain, J.; Plater, L.; Elliott, M.; Shpiro, N.; Hastie, C. J.; McLauchlan, H.; Klevernic, I.; Arthur, J. S.; Alessi, D. R.; Cohen, P. The selectivity of protein kinase inhibitors: A further update. *Biochem. J.* **2007**, *408*, 297−315.
(54) Fabian, M. A.; Biggs, W. H.; Treiber, D. K.; Atteridge, C. E.; Azimioara, M. D.; Benedetti, M. G.; Carter, T. A.; Ciceri, P.; Edeen, P. T.; Floyd, M.; Ford, J. M.; Galvin, M.; Gerlach, J. L.; Grotzfeld, R. M.; Herrgard, S.; Insko, D. E.; Insko, M. A.; Lai, A. G.; Lélias, J. M.; Mehta, S. A.; Milanov, Z. V.; Velasco, A. M.; Wodicka, L. M.; Patel, H. K.; Zarrinkar, P. P.; Lockhart, D. J. A small molecule-kinase interaction map for clinical kinase inhibitors. *Nat. Biotechnol.* **2005**, *23*, 329−336.
(55) Karaman, M. W.; Herrgard, S.; Treiber, D. K.; Gallant, P.; Atteridge, C. E.; Campbell, B. T.; Chan, K. W.; Ciceri, P.; Davis, M. I.; Edeen, P. T.; Faraoni, R.; Floyd, M.; Hunt, J. P.; Lockhart, D. J.; Milanov, Z. V.; Morrison, M. J.; Pallares, G.; Patel, H. K.; Pritchard, S.; Wodicka, L. M.; Zarrinkar, P. P. A quantitative analysis of kinase inhibitor selectivity. *Nat. Biotechnol.* **2008**, *26*, 127−132.
(56) Sharanin, Y. A.; Krivokolysko, S. G.; Dyachenko, V. D. Cyclization reactions of nitriles. LIV. Synthesis and properties of 6-amino-4-aryl-3,5-dicyanopyridin-2(1H)-ones, the corresponding thiones, the pyridylidenemalononitriles and their hydrogenated analogs. *Russ. J. Org. Chem.* **1994**, *30*, 620−626.
(57) Primot, A.; Baratte, B.; Gompel, M.; Borgne, A.; Liabeuf, S.; Romette, J. L.; Costantini, F.; Meijer, L. Purification of GSK-3 by affinity chromatography on immobilised axin. *Protein Expression Purif.* **2000**, *20*, 394−404.
(58) Kabsch, W. Software XDS for image rotation, recognition and crystal symmetry assignment. *Acta Crystallogr.* **2010**, *D66*, 125−132.
(59) McCoy, A. J.; Grosse-Kunstleve, R. W.; Adams, P. D.; Winn, M. D.; Storoni, L. C.; Read, R. J. Phaser crystallographic software. *J. Appl. Crystallogr.* **2007**, *40*, 658−674.
(60) Adams, P. D.; Afonine, P. V.; Bunkoczi, G.; Chen, V. B.; Davis, I. W.; Echols, N.; Headd, J. J.; Hung, L. W.; Kapral, G. J.; Grosse-Kunstleve, R. W.; McCoy, A. J.; Moriarty, N. W.; Oeffner, R.; Read, R. J.; Richardson, D. C.; Richardson, J. S.; Terwilligere, T. C.; Zwarta, P. H. PHENIX: A comprehensive Python-based system for macromolecular structure solution. *Acta Crystallogr.* **2010**, *D66*, 213−221.
(61) Emsley, P.; Lohkamp, B.; Scott, W. G.; Cowtan, K. Features and development of Coot. *Acta Crystallogr.* **2010**, *D66*, 486−501.
(62) Berman, H. M.; Westbrook, J.; Feng, Z.; Gilliland, G.; Bhat, T. N.; Weissig, H.; Shindyalov, I. N.; Bourne, P. E. The Protein Data Bank. *Nucleic Acids Res.* **2000**, *28*, 235−242.
(63) Brunger, A. T. Version 1.2 of the Crystallography and NMR system. *Nat. Protoc.* **2007**, *2*, 2728−2733.
(64) Rarey, M.; Kramer, B.; Lengauer, T. Multiple automatic base selection: Protein-ligand docking based on incremental construction without manual intervention. *J. Comput.-Aided Mol. Des.* **1997**, *11*, 369−384.
(65) Rarey, M.; Kramer, B.; Lengauer, T. The particle concept: Placing discrete water molecules during protein-ligand docking predictions. *Proteins* **1999**, *34*, 17−28.
(66) Rarey, M.; Kramer, B.; Lengauer, T.; Klebe, G. A fast flexible docking method using an incremental construction algorithm. *J. Mol. Biol.* **1996**, *261*, 470−489.
(67) Rarey, M.; Wefing, S.; Lengauer, T. Placement of medium-sized molecular fragments into active sites of proteins. *J. Comput.-Aided Mol. Des.* **1996**, *10*, 41−54.
(68) Reulecke, I.; Lange, G.; Albrecht, J.; Klein, R.; Rarey, M. Towards an integrated description of hydrogen bonding and dehydration: Decreasing false positives in virtual screening with the HYDE scoring function. *ChemMedChem* **2008**, *3*, 885−897.
(69) Dzikowski, R.; Frank, M.; Deitsch, K. Mutually exclusive expression of virulence genes by malaria parasites is regulated independently of antigen production. *PLoS Pathog.* **2006**, *2*, e22.